Room temperature mid-infrared InAsSbN multi-quantum well photodiodes grown by MBE

You may also be interested in:

Room temperature mid-infrared InAsSbN multi-quantum well photodiodes grown by MBE

M Kesaria, M de la Mare and A Krier

Physics Department, Lancaster University, Lancaster, LA1 4YB, UK

E-mail: m.kesaria@lancaster.ac.uk

CrossMark

Abstract

Room temperature photoresponse in the mid-infrared spectral region is demonstrated from InAsSbN/InAs multi-quantum well photodiodes grown by nitrogen plasma assisted molecular beam epitaxy. The structural quality of the InAsSbN MQWs was ascertained *in situ* by reflection high energy electron diffraction and *ex situ* by high resolution x-ray diffraction and photoluminescence measurements. The extended long wavelength photoresponse is identified to originate from the electron–heavy hole (e_1–hh_1) and electron–light hole (e_1–lh_1) transitions in the InAsSbN MQW, with a cut off wavelength ~4.20 μm and peak detectivity $D^* = 1.25 \times 10^9$ cm Hz$^{1/2}$ W^{-1}.

Keywords: dilute nitride, InAsSbN, MBE, photodiodes

(Some figures may appear in colour only in the online journal)

Introduction

Photodetectors operating in the mid-infrared spectral range (3–5 μm) are of technological importance due to their military applications in infrared countermeasures and night vision as well as many civil applications, including atmospheric pollution monitoring, optical spectroscopy and medical diagnostics. Mercury cadmium telluride (MCT) photodetectors are commonly used for some of these applications together with InGaAs, InSb, InAsSb [1] and InAsSbP [2]. MCT alloys have a small electron effective mass (~0.009 m_0) resulting in undesirable dark currents due to tunnelling and require cooling. These alloys also suffer from compositional non-uniformity which compromises the detector spectral response over large areas [3–5]. Access to mid-infrared wavelengths can also be achieved using alternative III–V based material systems such as InAsN, where the addition of small amounts (<1%) of nitrogen into InAs has been found to substantially reduce the band gap and allow tailoring of the detection wavelength

[6–9]. Research into dilute nitride materials can give insight into fundamental physics and also has potential for the development of new high performance detectors and large-format focal plane arrays [10, 11].

Room temperature electroluminescence (EL) at a peak wavelength ~3.7 μm was demonstrated earlier from type II InAsSb/InAs multi-quantum well (MQW) light-emitting diodes (LEDs) [12]. The introduction of nitrogen into InAsSb quantum wells changes the band alignment from type-II to type-I due to an increase in the electron confinement and bandgap reduction, with no excess strain. The surfactant effect of Sb during growth enhances the crystalline and optical quality of InAsSbN, whereas the adjustment of Sb and N contents enables lattice matching to InAs and strain tailoring in the QW. Previously, we have reported good quality InAsSbN alloys, InAsSbN p-i-n diodes emitting near 4.0 μm at room temperature [13–15], InAsSbN MQW [16] and InAsSbN MQW LEDs emitting at 3.6 μm (4 K) [17]. More recently InAsN and InGaAsN MQW implemented on InP substrate have been shown to enable dilute nitride mid-infrared laser diodes [18]. InAsSbN quantum wells [19] and laser diodes [20] have also been reported elsewhere in the literature, but there are very few studies

(a)
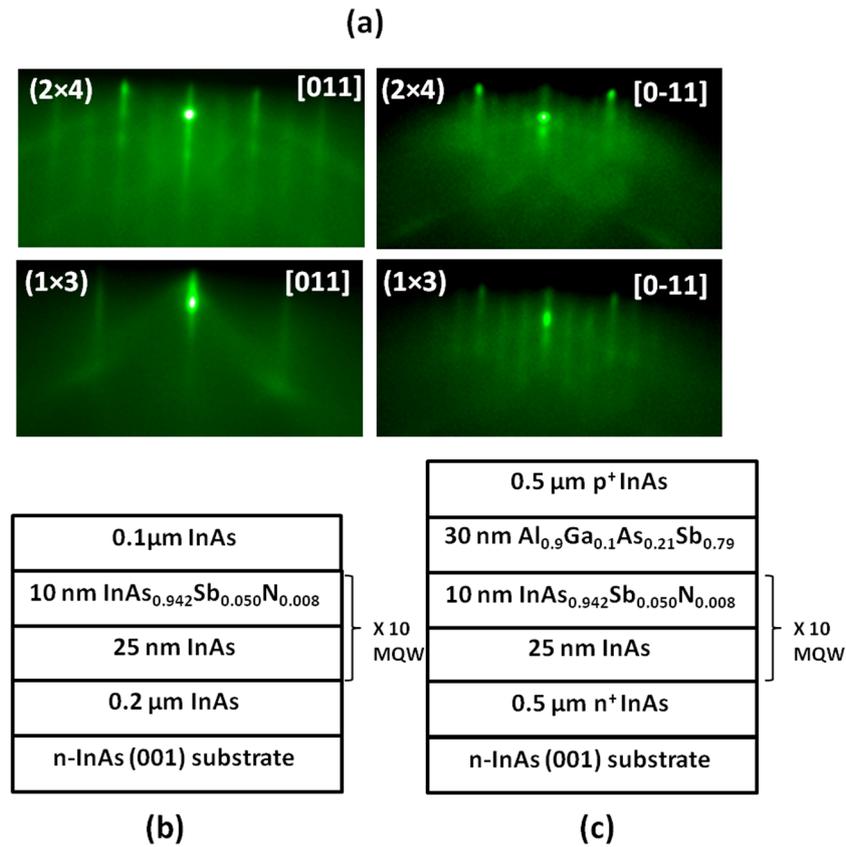
Figure 1. (a) Typical 2 × 4 and 1 × 3 RHEED patterns for InAs and InAsSbN surface observed during the growth in the [0 1 1] and the [0 1 1] direction; (b) schematic details of the MQW structure used in the photodiode active region and (c) the complete photodiode structure, each containing 10 InAsSbN quantum wells.

on dilute nitride photo-detectors operating in the 2–5 μm spectral range [21–23].

In this work, we demonstrate InAsSbN MQW photodiodes grown on InAs substrate by plasma assisted molecular beam epitaxy. The structural quality of the InAsSbN MQWs was ascertained by high resolution x-ray diffraction and photoluminescence measurements. Room temperature photoresponse was observed in the mid-infrared, with a cut-off wavelength near 4.20 μm and a peak detectivity of $D^* = 1.25 \times 10^9$ cm Hz$^{1/2}$ W^{-1}. The extended long wavelength response was identified to originate from confined states of the dilute nitride MQW (e_1–hh_1 and e_1–lh_1) which is in good agreement with calculated values.

Experiment

A VG-V80H molecular beam epitaxy (MBE) reactor was used to grow the InAsSbN quantum wells on *n*-InAs (0 0 1) substrates, as well as the complete MQW photodiode device structure. During this growth phase, *in situ* characterization was performed by reflection high energy electron diffraction (RHEED). In, Al and Ga fluxes were provided by Knudsen thermal effusion cells. The As$_2$ and Sb$_2$ was generated from valved cracker cells and the atomic N flux by a Veeco Uni-bulb radio frequency plasma nitrogen source. The nitrogen flux was generated using a load power of 210 W

and a nitrogen beam equivalent pressure (BEP) ~ 7.0×10^{-7} mbar. BEP ratio of As/Sb = 2.6 and As/N = 3.7 (BEP of Sb ~ 1.1×10^{-6} mbar, BEP of N$_2$ ~ 7.0×10^{-7} mbar and As ~ 2.6×10^{-6} mbar). To optimize N incorporation into the MQW the minimum As flux was used during the growth of the InAs layers, since the adatom sites are more favourable for As than for N incorporation. In order to ascertain surface cleanliness and monitor crystalline quality, surface reconstructions were monitored by RHEED. Typical (2 × 4) and (1 × 3) RHEED patterns shown in figure 1(a) were observed during the growth in [0 1 1] and [0 1 1] directions for the InAs and InAsSbN surfaces, respectively. The substrate temperature was measured using an infrared pyrometer and back-calibrated by monitoring surface reconstruction transitions at a fixed As flux. The substrate preparation and oxide desorption was carried out in the conventional manner in the growth chamber. To desorb oxide from the InAs substrate required heating gradually up to 520 °C under As flux, (until a weak × 3 RHEED pattern transformed to the brighter × 2 pattern) [24]. To obtain abrupt quantum well interfaces and realize a low residual carrier concentration ~2×10^{17} cm^{-3} in the MQW, the surface was exposed to Sb for 3s (Sb flux ~3×10^{-7}) prior to InAsSbN quantum well growth and before the InAs barrier growth the surface was exposed to As (flux ~4×10^{-6} mbar) for 20 s. The RHEED pattern was clearly 1 × 3 at the beginning of the active region and transformed to 2 × 4 under As$_2$ flux, suggesting an efficient As–Sb exchange
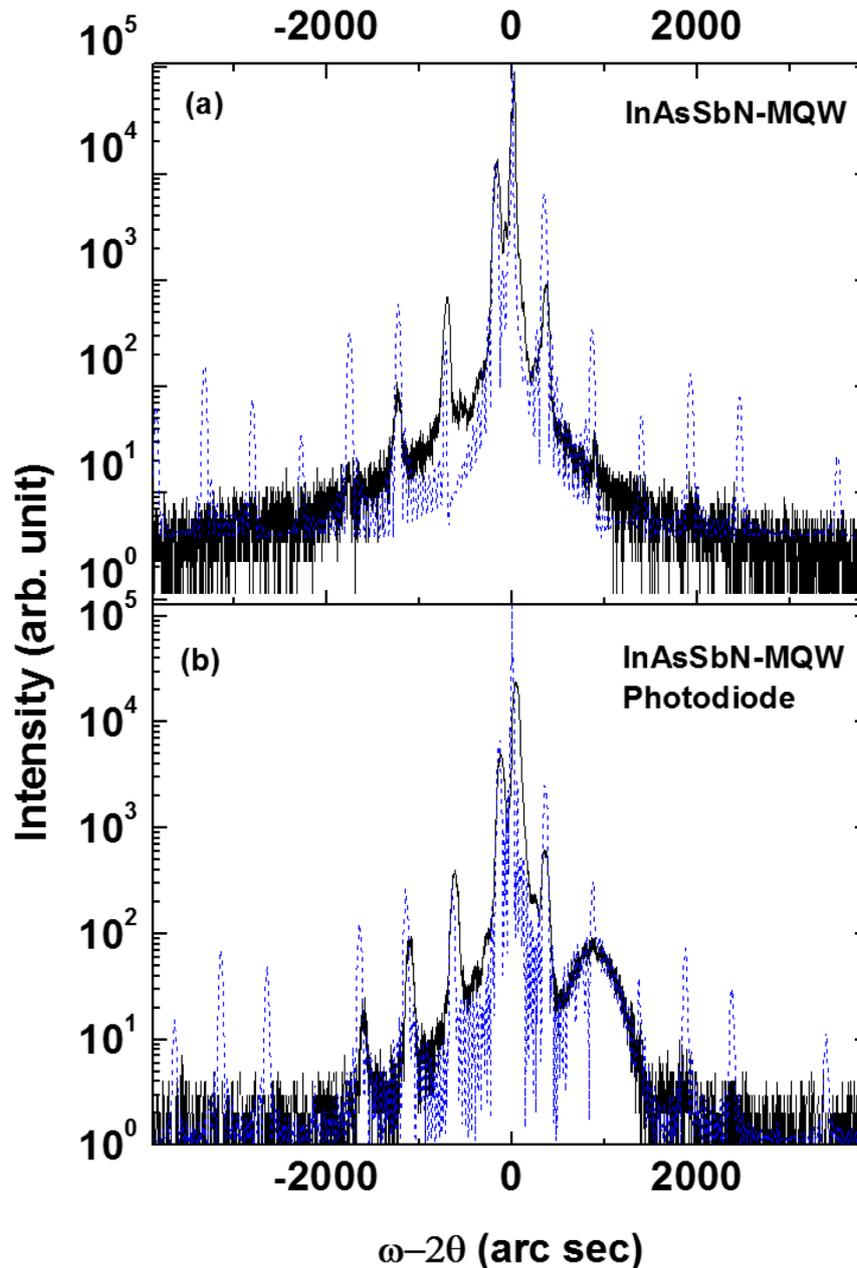
Figure 2. High resolution x-ray diffraction rocking curves (black) and simulated XRD patterns (blue dotted) of (a) the MQW active region and (b) the complete photodiode structure.

reaction and excess Sb removal from the surface. The structural quality and material composition was determined using high resolution x-ray diffraction (HRXRD) measurements. The resulting wafers were processed into 1 mm diameter mesa-etched diodes using standard photolithographic and wet etching techniques before mounting onto TO-46 headers. Photoluminescence (PL) and electroluminescence (EL) measurements were performed using an Oxford Instruments variable temperature continuous flow He cryostat. The emitted radiation was collected using CaF_2 lenses and focused into a 0.3 m Bentham M300 grating monochromator. For EL the devices were tested at 1 kHz using a 50% duty cycle excitation and the radiation was detected using a cooled (77 K) InSb photodiode detector and a Stanford Research (SR850)

digital lock-in amplifier. The photo-response was measured using an Oriel Instruments 80007 silicon carbide source with a 1200 K colour temperature that was chopped at 175 Hz.

A schematic representation of the MQW structure and the corresponding photodiode detector is shown in figures 1(b) and (c), respectively. The MQW structure consists of ten $InAs_{0.942}Sb_{0.050}N_{0.008}$ quantum wells, each 10 nm wide with 25 nm InAs barriers, grown on InAs substrate. For the photodiode a 0.5 μm Te doped InAs layer is grown on InAs at 490 °C (1 μm h^{-1} growth rate) which is followed by ten 10 nm $InAs_{0.942}Sb_{0.050}N_{0.008}$ quantum wells with 25 nm InAs barriers (0.5 μm h^{-1} growth rate) at lower substrate temperature 410 °C. The growth temperature is raised to 490 °C for the growth of the 30 nm undoped $Al_{0.90}Ga_{0.10}As_{0.21}Sb_{0.79}$ electron

J. Phys. D: Appl. Phys. **49** (2016) 435107

M Kesaria *et al*
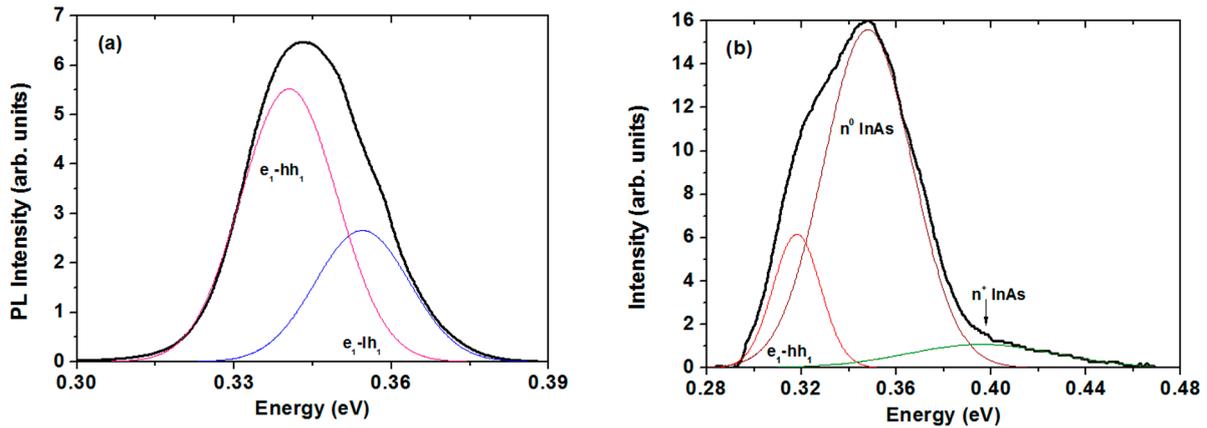
Figure 3. (a) The 4 K PL spectra and (b) 300 K EL spectra in black. The de-convoluted Gaussian peaks; e_1–hh_1 (red), e_1–lh_1 (blue), n^0 InAs (brown) and n^+ InAs (green) are labelled accordingly.

blocking barrier above the active region and finally capped by 500 nm thick Be-doped InAs.

Results and discussion

The incorporation of N or Sb into InAs layers is known to introduce tensile or compressive strain respectively. Therefore, addition of 0.8% N to $InAs_{0.95}Sb_{0.05}$ MQW reduces compressive strain from 0.5% to 0.2% allowing strain-balancing and we used this in the growth of the InAsSbN MQW structure and photodiode used here. The corresponding HRXRD rocking curves are shown in figures 2(a) and (b), respectively. The peak at 858 arc seconds corresponds to the $Al_{0.90}Ga_{0.10}As_{0.21}Sb_{0.79}$ layer in the photodiode. The diffraction pattern of both structures has a distinct zero order peak and a few high-order satellite peaks. The absence of higher angle satellite peaks can be due to atomic level roughness at the interface between the well and barrier. In our earlier work we have shown that in InAsSbN/ InAs MQWs the interface between the well and barrier can have roughness up to ±2 nm [17]. InAsSbN epilayers (1 μm thick) grown on InAs substrate in different Sb and N conditions were used to determine Sb and N composition [14–16]. Simulation of the structures was done using Bede RADS software which is based on the dynamical scattering theory of diffraction. The solid lines (black) are experimental results and the dashed lines (blue) are simulated data. The derived thicknesses of the perfectly strain balanced InAsSbN well and InAs barrier are approximately 10 nm and 25 nm, respectively.

Figure 3 shows (a) the 4 K PL emission spectrum and (b) the 300 K EL spectrum. The experimental PL and EL data were de-convoluted by fitting Gaussian peaks. For the 4 K PL these peaks are centred at 0.340 and 0.355 eV, which is approximately in agreement with the calculated e_1–hh_1 and e_1–lh_1 QW transitions, respectively. The calculation of the transition energies was done using a Schrodinger solver within an effective mass approximation, taking into account N-induced band anti-crossing effects, coupling constants and strain [16]. The difference between calculated and experimental values originates from uncertainties in N and Sb content and also the effective masses within the QW [25]. The room temperature EL spectrum shown in figure 3(b) was similarly de-convoluted
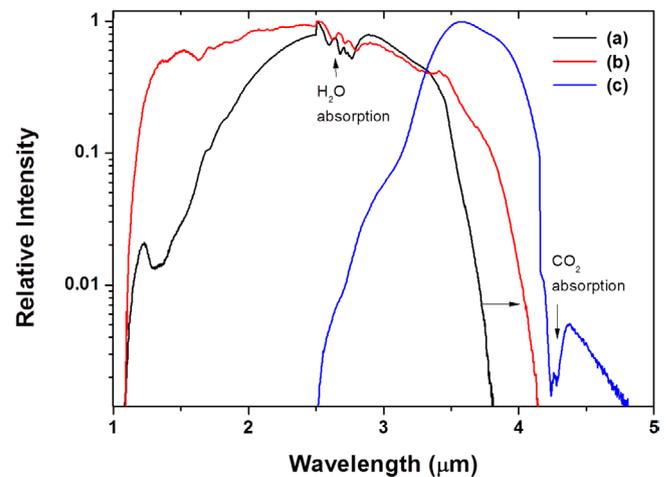

Figure 4. The room temperature logarithmic plots of (a) photoresponse from a bulk InAs photodiode with an InAsSbP window, (b) the InAsSbN MQW photodiode and (c) electroluminescence from the InAsSbN MQW diode (at injection current 100 mA). The photoresponse spectra contain features due to atmospheric absorption from water vapour in the optical path around 2.7 μm.

into three peaks which are centred at 0.318 eV, 0.349 eV and 0.396 eV. The first being attributed to e_1–hh_1 QW transition, while the peaks at 0.349 eV and 0.396 eV arises from recombination taking place in the intrinsic n^0 InAs barriers and n^+ InAs, respectively.

Figure 4 compares the room temperature photoresponse of (a) an InAs photodiode (with an InAsSbP window) [26], (b) the InAsSbN MQW photodiode, and (c) the electroluminescence from the InAsSbN MQW diode. The photoresponse of the InAsSbN MQW photodiode extends from 1.10 to 4.20 μm having an extended cut off at 4.20 μm compared with the cut off wavelength for InAs at 3.88 μm. The maximum of the electroluminescence spectrum at 3.57 μm is 0.63 μm lower than the cut-off of the MQW diode photoresponse.

Current–voltage (*I–V*) curves were obtained at temperatures 20 K–300 K for the InAsSbN MQW photodiode. Figure 5(a) shows a semi-logarithmic plot of the *I–V* curves acquired at 20, 160 and 300 K using a bias in the range −0.4 to 0.8 V from which the corresponding diode series resistance is estimated

J. Phys. D: Appl. Phys. 49 (2016) 435107

M Kesaria *et al*
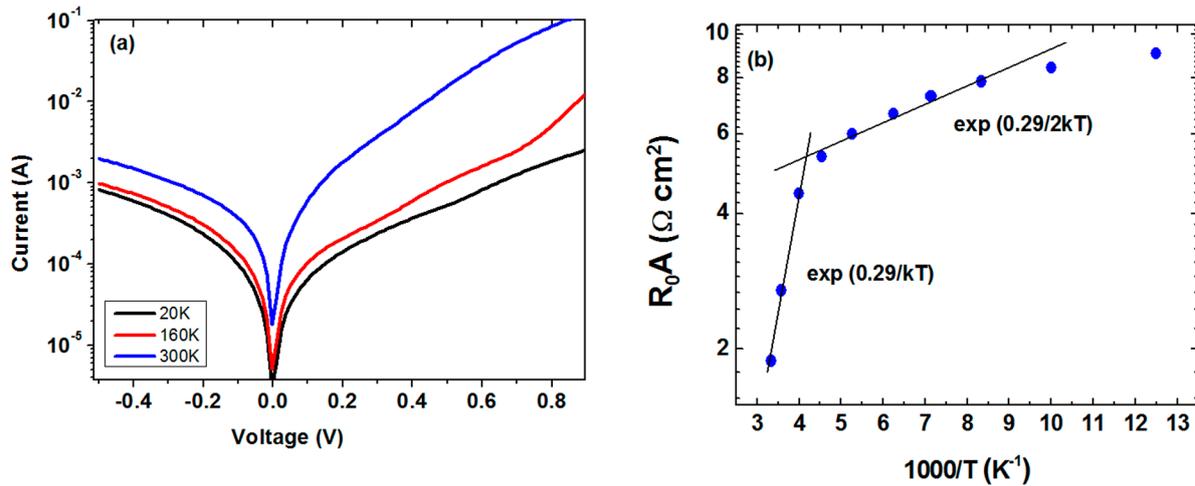
Figure 5. (a) The *I–V* curves acquired at 20 K, 160 K and 300 K from the InAsSbN MQW photodiode (data for other temperatures omitted for clarity); and (b) the zero bias resistance area (R_0A) versus reciprocal of temperature plot derived from the *I–V* measurements for the same InAsSbN diode. The straight lines correspond to $\exp(0.29/kT)$ and $\exp(0.29/2kT)$.

as ~2.5 Ω and the ideality factor (β) ~1.56 below 150 K. The diode reverse leakage current decreased from 2 mA to 0.7 mA with a reduction in temperature from 300 K to 20 K. To understand the current conduction mechanisms an Arrhenius plot of zero bias resistance area (R_0A) was extracted and is shown in figure 5(b). The R_0A values grow exponentially with decreasing temperature, but the growth rate is different at high and low temperatures. The straight lines show the fits obtained using the energy ($E = 0.29$ eV) in the exponent ($\exp E/\beta kT$) which is close to the e$_1$–hh$_1$ transition of the InAsSbN ($N \sim 1\%$) MQWs. The results are consistent with diffusion current ($\beta \sim 1$) in the 200–300 K temperature range. At low temperatures generation recombination current dominates consistent with $\beta \sim 2$. The specific (peak) detectivity of the InAsSbN MQW photodiode was determined as $D^* = 1.25 \times 10^9$ cm Hz$^{1/2}$ W^{-1} at 300 K for the mesa etched 1 mm diameter diodes in this work, using the Johnson noise limited equation [27]. This is comparable with previously reported InAsSb (InAsSbP) photodiodes at 300 K [1–2] and is encouraging since the MQW diodes are not yet optimized or anti-reflection coated. The valence band offsets (62 meV) of the MQWs are small enough to allow the photogenerated carriers to escape at 300 K and the number of QW can be increased further to increase absorption using strain balancing. Consequently, this material system shows promise as the addition of N provides an additional freedom in tailoring the band structure within a type I QW system at longer wavelengths. To improve device quality, further work is in progress to reduce the active region residual carrier concentration and improve the MQW interface quality as well as extend the wavelength range by the introduction of more nitrogen.

Conclusion

We have demonstrated uncooled InAsSbN/InAs MQW photodiodes, grown strain balanced on InAs by MBE, which exhibit a photoresponse in the mid-infrared spectral range at 300 K.

The structural and optical quality were ascertained by high resolution x-ray diffraction and photo-/electroluminescence. The diodes exhibit responsivity in the mid infrared spectral region with an extended long wavelength response, which is identified to originate from the InAsSbN e–hh$_1$ and e–lh$_1$ transitions and is in agreement with calculated values. The photodiodes exhibit a cut-off wavelength of near 4.2 μm at room temperature with a specific detectivity, $D^* = 1.25 \times 10^9$ cm Hz$^{1/2}$ W^{-1} at 300 K. Since InAsSbN enables strain-balancing on InAs the dilute nitride alloys offer some additional freedom in tailoring long wavelength photodetectors.

References

[1] Gao H H, Krier A and Sherstnev V V 2000 *Appl. Phys. Lett.* **77** 872
[2] Krier A and Suleiman W 2006 *Appl. Phys. Lett.* **89** 083512
[3] Rogalski A 2005 *Rep. Prog. Phys.* **68** 2267
[4] Rogalski A 2012 *Opto-Electron. Rev.* **20** 279
[5] Rogalski A 2010 *Opto-Electron. Rev.* **18** 478
[6] Nishikawa A, Katayama R, Onabe K and Shiraki Y 2003 *J. Cryst. Growth* **251** 427
[7] Ding-Kang S, Hao-Hsiung L, Li-Wei S, Tso-Yu C and Yang T R 2003 *Japan. J. Appl. Phys.* **42** 375
[8] Bi W G and Tu C W 1997 *Appl. Phys. Lett.* **70** 1608
[9] Chang A S, Zech E S, Kim T W, Lin Y H, Mawst L J and Goldman R S 2014 *Appl. Phys. Lett.* **105** 142105
[10] Veal T D, Piper L F J, Jefferson P H, Mahboob I, McConville C F, Merrick M, Hosea T J C, Murdin B N and Hopkinson M 2005 *Appl. Phys. Lett.* **87** 182114
[11] Kuroda M, Katayama R, Nishio S, Onabe K and Shiraki Y 2003 *Phys. Status Solidi* c **0** 2765

[12] Krier A, Stone M, Zhuang Q D, Liu P-W, Tsai G and Lin H H 2006 *Appl. Phys. Lett.* **89** 091110

[13] Zhuang Q, Godenir A, Krier A, Tsai G and Lin H H 2008 *Appl. Phys. Lett.* **93** 121903

[14] Latkowska M *et al* 2016 *J. Phys. D: Appl. Phys.* **49** 115105

[15] Godenir A 2008 Novel dilute nitride semiconductor materials for mid-infrared applications *PhD Dissertation* Lancaster University, Lancaster (available from: Lancaster E-prints)

[16] de la Martin M, Carrington P J, Wheatley R, Zhuang Q, Beanland R, Sanchez A M and Krier A 2010 *J. Phys. D: Appl. Phys.* **43** 345103

[17] Carrington P J, de la Mare M, Cheetham K J, Zhuang Q and Krier A 2011 *Adv. OptoElectron.* **2011** 145012

[18] Wheatley R, Kesaria M, Mawst L J, Kirch J D, Kuech T F, Marshall A, Zhuang Q D and Krier A 2015 *Appl. Phys. Lett.* **106** 232105

[19] Shono T, Mizuta S and Kawamura Y 2013 *J. Cryst. Growth* **378** 69

[20] Kawamura Y and Inoue N 2007 *J. Cryst. Growth* **301–2** 963

[21] Tan K H *et al* 2007 *Appl. Phys. Lett.* **90** 183515

[22] Luna E, Hopkinson M, Ulloa J M, Guzmán A and Muñoz E 2003 *Appl. Phys. Lett.* **83** 3111

[23] Aina L, Hier H, Fathimulla A, Lecates M, Kolodzey J, Goossen K, Coppinger M and Bhargava N 2009 *Infrared Phys. Technol.* **52** 310

[24] Bhatnagar K, Rojas-Ramirez J, Caro M, Contreras R, Henninger B and Droopad R 2015 *J. Cryst. Growth* **425** 16

[25] Patanè A *et al* 2009 *Phys. Rev.* B **80** 115207

[26] Krier A *et al* 2015 *Infrared Phys. Technol.* **73** 126

[27] Dennis P N J 1986 *Photodetectors* (New York: Plenum)